Sensors & Transducers, Vol. 183, Issue 12, December 2014, pp. 192-196

Sensors & Transducers

http://www.sensorsportal.com

Numerical and Experimental Study of Amplitude Modulated Positive Corona Discharge

[1] Pablo Martín GOMEZ, [2] Guillermo SANTIAGO

[1] Laboratorio de Acústica y Electroacústica (LACEAC), Departamento de Electrónica, Facultad de Ingeniería, Universidad de Buenos Aires, Paseo Colón 850, C1063ACV, Buenos Aires

[2] Grupo de Láser, Óptica de Materiales y Aplicaciones Electromagnéticas (GLOMAE), Departamento de Física, Facultad de Ingeniería, Universidad de Buenos Aires, Paseo Colón 850, C1063ACV, Buenos Aires, Argentina

[1] Tel.: 54 11 4343 0891

[1] E-mail: elpablogomez@gmail.com

Received: 27 October 2014 /Accepted: 28 November 2014 /Published: 31 December 2014

Abstract: The electrical behavior of a modulated positive corona discharge loudspeaker was studied. A coaxial transducer in air was built using a central copper wire of 75 μm radius (inner electrode) and a perforated tube of 11 mm (outer electrode). A high voltage DC supply provided the bias current and a sinusoidal signal was superimposed to measure the discharge admittance. The experimental results could not be matched to previously reported equivalent circuits with fixed components. Using the basic equations that describe the ion motion, a numerical model was proposed. The computed values matched well the experimental data and suggested an equivalent circuit composed of frequency dependent conductance and capacitance. This dependence is closely related to the ion travel time between electrodes (transit time). Simulations carried out at several inter-electrode distances could be synthesized in a single plot where the different results overlap and further emphasize the role of the transit time. This numerical model proved to be an efficient tool to simulate and design modulated corona transducers.

Keywords: Corona discharge, Transducers, Numerical model, Equivalent circuits, Ionic current.

1. Introduction

Corona discharge loudspeakers, despite their low efficiency are interesting tools in audio research because they are capable of generating complex wavefronts; a fact not easily attainable with standard loudspeakers. We resorted to this flexibility to build a cylindrical wavefront transducer. In order to develop its electroacoustic model we measured, as a first step, the electrical properties of the discharge.

Previous works [1-4] point out the corona discharge can be modeled by an equivalent electrical circuit composed of fixed resistors (dependent on carrier densities) and a capacitor. However, when we attempted to fit the measured admittance to this equivalent model the results were disappointing: some components should have had negative values. This discrepancy prompted us to carry out a numerical simulation of the corona discharge that includes the basic physical phenomena that govern the ion motion.

The numerical outcome fits well with experimental results and show the conductance and capacitance vary with frequency in a complex way. This explains our previous failure to find an equivalent circuit based on fixed components. In

addition we found the response at different electrode distances can be summarized in a single one, by taking into account the finite ion velocity.

2. Experimental Setup

A scheme of the transducer and driving circuit is depicted in Fig. 1. The inner electrode is a thin copper wire with radius a = 75 μm and the outer one is a perforated tube with inner radius b = 11 mm. The total length of the prototype is one meter.

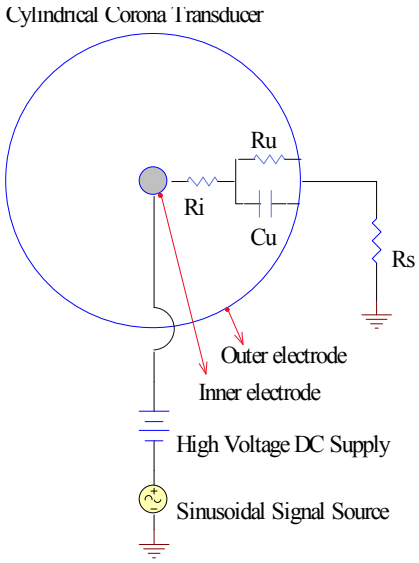

Fig. 1. Scheme of the transducer and driving circuit.

A variable high voltage DC supply (V_{DC} = 0 - 15 kV) ionizes the air and determines a bias current I_{DC} given by:

$$I_{DC} = c\,V_{DC}(V_{DC} - V_0), \tag{1}$$

where c is the constant that depends on the shape, the dimensions and the gas and V_0 is the threshold voltage. The static curve of the prototype is shown in Fig. 2.

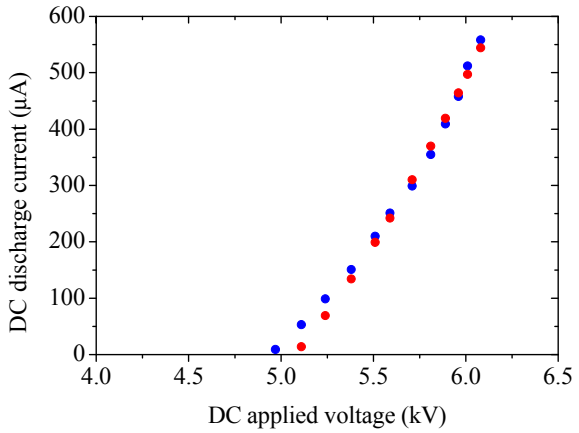

Fig. 2. Static curve of the transducer: Blue – Experimental; Red – Numerical.

The sinusoidal signal source (V_{AC} = 0 - 150 V_{rms}) modulates the applied voltage around its mean value (4 to 20 kHz), thus achieving a variable current (I_{AC}) which in turn, generates sound [1]. The sampling resistor R_s (1 kΩ) serves to acquire the discharge current. The voltage drop across R_s is low enough to consider the outer electrode is grounded. A high voltage probe connected to the inner electrode monitors the applied voltage. The complex ratio of I_{AC} to V_{AC} defines the input admittance. A typical result is presented in Fig. 3(a) and Fig. 3(b). As mentioned in the introduction, the experimental results could not be matched to the standard equivalent circuit of Fig. 1. R_i is related to the ionization sheath, R_u to the ion drift zone and C_u is the inter-electrode capacitance.

3. Numerical Model and Simulation

3.1. Numerical Model

To comprehend these differences, we simulated the amplitude modulated corona discharge in COMSOL Multiphysics®, considering the following equations:

$$\vec{J} = \rho\vec{v} + \varepsilon_0 \frac{\partial \vec{E}}{\partial t}, \tag{2}$$

$$-\nabla^2\Phi = \frac{\rho}{\varepsilon_0}, \tag{3}$$

$$\vec{v} = \mu\vec{E}, \tag{4}$$

$$\vec{\nabla} \bullet \vec{J} = -\frac{\partial \rho}{\partial t}, \tag{5}$$

where J is the current density, ε_0 is the vacuum permitivity, ρ is the charge density, v is the ion drift velocity, μ is the ion mobility (2×10^{-4} m^2/Vs), E is the electric field and Φ is the electric potential. In the continuity Eq. (5) J does not include the displacement current. These equations have already been considered by Janischewskyj *et al* [5] except for the time varying terms.

By applying straightforward substitutions we reduced the problem to two coupled partial derivative equations with dependent variables Φ and ρ. Owing to the symmetry of the problem it can be cast as a one dimensional model in the independent radial variable r and time t.

The boundary conditions at the inner electrode are: a potential $\Phi(a) = V_{DC} + V_{AC}$ and an electric field E derived from Kaptzov's assumption [6] which states the field, at the corona electrode, is always equal to the onset value E_0 derived from Peek's experimental equation in air [7]:

$$E_0 = 3.1\times10^6\left(1+\frac{0.308}{\sqrt{0.5\times a}}\right)\ \text{(V/m)}, \tag{6}$$

where a is the wire radius in meters.

As a consequence of choosing independent values of Φ and E at the inner electrode, the charge density ρ must be compatible with those conditions.

Kaptzov's assumption strictly applies to a stationary regime and has been used to simulate in depth DC discharges [8]. However, the same assumption has been employed to describe pulsed electrostatic precipitators [9].

The model neglects any voltage drop across the ionization sheath. This makes R_i negligible compared with the parallel of R_u and C_u. The validity of such an assumption will be given by the experiment.

As a first test, by setting $V_{AC} = 0$, we checked the numerical model reproduces the static curve. This is shown in Fig. 2. At very low currents the measured values depart from the computed ones. The differences could be traced down to corona discharge fluctuations ("flashing corona") [10].

3.2. Modulated Corona Discharge

Afterwards, we ran the simulation at different frequencies and a constant AC signal voltage. The computed admittance modulus and phase are displayed in Fig. 3(a) and Fig. 3(b) respectively, together with the measured data. The agreement is quite good despite the "phase undulations" did not appear in the experimental results.

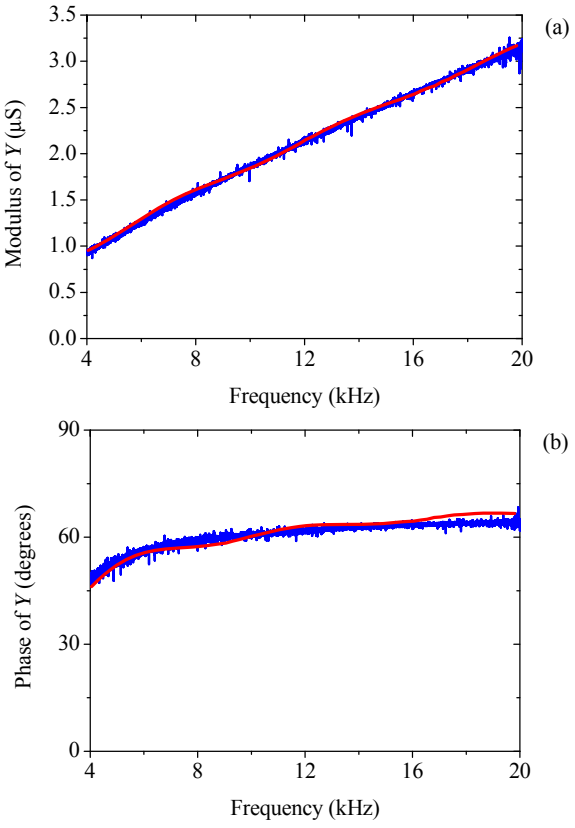

Fig. 3. Admittance: (a) modulus, (b) phase. I_{DC} = 500 μA, V_{AC} = 70 V_{rms}. Blue – Experimental; Red – Numerical.

The results hint the assumption of no voltage drop across the ionization sheath holds well. Therefore, the real part of the admittance can be considered as the dynamic conductance of the discharge. The same happens with the imaginary part which brings the equivalent capacitance, computed as the ratio of the imaginary part to ω. See, Fig. 4 (a) and Fig. 4 (b).

It can be seen both magnitudes vary with frequency in a complex way. Thus, if a simple parallel RC circuit is desired, frequency dependent components must be allowed. Owing to the complexity of the differential equations, finding an analytical solution is too difficult and the dependence of the components on frequency is available through the simulation.

The average capacitance in the range from 4 to 20 kHz is about 23 pF, a value above the geometrical one (11 pF). The extra capacitance can be ascribed to the space charge which varies in each cycle around its mean value.

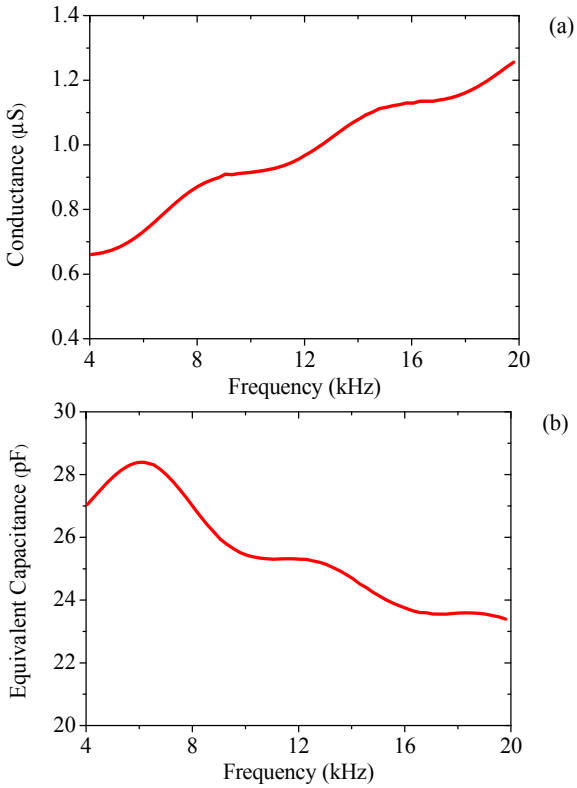

Fig. 4. (a) Discharge conductance, (b) Discharge equivalent capacitance.

Having checked the simulation, we ran it again at different inter-electrode distances to analyze the effects of the finite ion velocity (Fig. 5). From here on, we present phase plots as they show subtle details not easily appreciable in the modulus ones. Although the results look unrelated, it is possible to bring them together by considering a new variable: the transit time (τ_{tr}) defined as the elapsed time since an ion leaves the ionization sheath until it reaches the outer electrode. It is computed as:

$$\tau_{tr} = \int dt = \int \frac{dr}{v(r)} = \int \frac{dr}{\mu E(r)}, \qquad (7)$$

where a is the wire radius and E refers to the DC electric field value.

The product of ω and τ_{tr} is usually known as the transit angle θ [11]. Now, if Fig. 5 is plotted as a function of θ, the different simulations overlap showing the influence of the finite ion velocity on the behavior of the corona discharge admittance (Fig. 6). This figure summarizes the admittance phase behavior of the discharge evaluated at different inter-electrode distances.

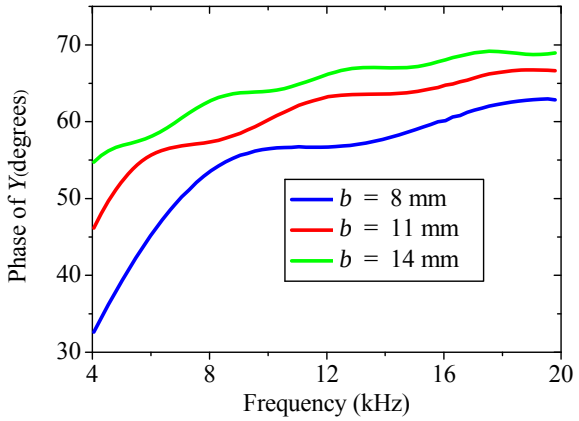

Fig. 5. Admittance phase vs. frequency for different outer electrode radius. I_{DC} = 500 µA, V_{AC} = 70 V_{rms}.

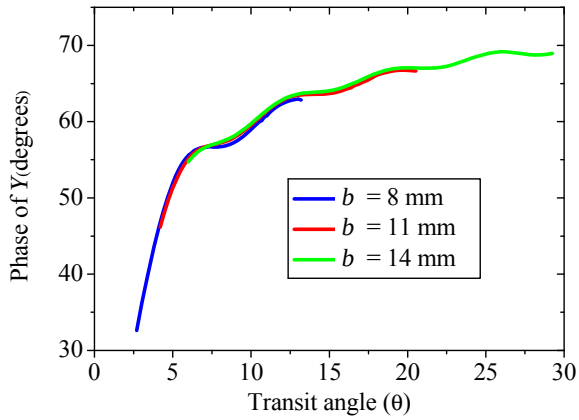

Fig. 6. Admittance phase vs. transit angle θ for different outer electrode radius. I_{DC} = 500 µA, V_{AC} = 70 V_{rms}.

To emphasize the role of the slowly moving ions we ran a simulation assuming a Gaussian pulse input voltage (amplitude = 100 V, pulse width = 20 µs FWHM). We chose a pulse length much shorter than the transit time in order to visualize the delay between the excitation and the ions arrival at the outer electrode. The results are presented in Fig. 7. At the time the pulse is applied, a corresponding current one appears because of the increased electric field that speeds up the ions close to the outer electrode. Another current signal shows up some time later. This corresponds to a "charge packet" produced at the inner electrode to fulfill Kaptzov's assumption. The time delay between the two current pulses is almost equal to the transit time. Clearly the ionic current does not follow instantaneously the applied voltage, therefore, it is not possible to assign a simple resistor as a circuital equivalent of the ion transport across the inter electrode gap.

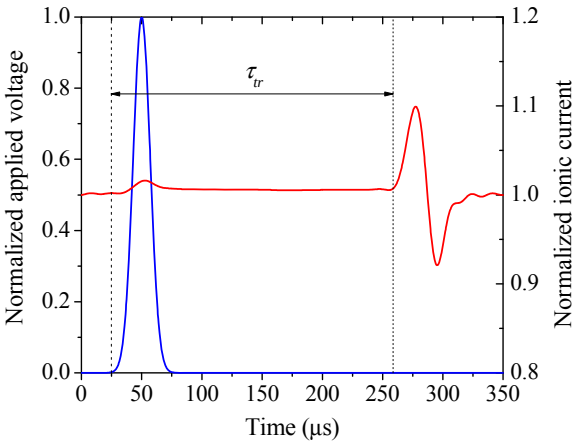

Fig. 7. Normalized applied voltage (blue) and ionic current at the outer electrode (red). $\tau_{tr} \approx$ 235 µs. I_{DC} = 500 µA. b = 14 mm.

4. Conclusions

The numerical and experimental results shows good agreement and point out the AC modulated positive corona discharge cannot be modeled by a simple parallel RC circuit with fixed components. It is possible to describe the discharge in terms of frequency varying conductance and capacitance connected in parallel. This dependence can be traced down to the finite ion velocity. By defining a transit time in terms of that velocity, it is possible to find the electrical response independently of the distance between electrodes.

The proposed numerical model not only is useful to analyze corona loudspeakers, but also in pulsed systems such as electrostatic precipitators.

Acknowledgements

The authors wish to thank COMSOL Inc. and Jonathan Velasco for their support. During the free workshops held at Buenos Aires in 2014, the authors acquired simulations skills and were granted a fully-functional software trial.

This work was supported by Project UBACyT 20020120100025 and the Electronics Department of the School of Engineering at the University of Buenos Aires.

References

[1]. Ph. Béquin, K. Castor, Ph. Herzog, V. Montembault, Modelling plasma loudspeakers, *Journal of the Acoustic Society of America*, Vol. 121, Issue 4, 2007, pp. 1960-1970.

[2]. Ph. Béquin, V. Montembault, Ph. Herzog, Modelling of negative point-to-plane corona loudspeaker, *The European Physical Journal Applied Physics*, Vol. 15, Issue 1, 2001, pp. 57–67.

[3]. M. M. Kekez, P. Savic, G. D. Lougheed, A novel treatment of Trichel type phenomena with possible application to stepped-leader phenomena, *Journal of Physics D: Applied Physics*, Vol. 15, Issue 10, 1982, pp. 1963–1973.

[4]. K. Matsuzawa, Sound sources with corona discharges, *Journal of the Acoustic Society of America*, Vol. 54, Issue 2, 1973, pp. 494-498.

[5]. W. Janischewskyj, G. Gela, Finite element solution for electric fields of coronating DC transmissions lines, *IEEE Transactions on Power Apparatus and Systems*, Vol. PAS-98, Issue 3, 1979, pp. 1000-1012.

[6]. N. A. Kaptzov, Electrical phenomena in gases and vacuum, *OGIZ*, 1947 (in Russian)

[7]. F. W. Peek, Dielectric Phenomena in High Voltage Engineering, *McGraw-Hill*, 1929.

[8]. K. Adamiak, P. Atten, Simulation of corona discharge in point-plane configuration, *Journal of Electrostatics*, Vol. 61, Issue 2, 2004, pp. 85-98.

[9]. Z. M. Al-Hamouz, Finite element computation of electric field and charge density of a pulsed energized electrostatic precipitator, in *Proceedings of the IAS Annual Meeting (IEEE Industry Applications Society)*, Chicago, United States, 30 September – 4 October 2001, pp. 2693-2698.

[10]. Y. P. Raizer, Gas discharge physics, *Springer-Verlag*, 1991.

[11]. F. B. Llewellyn, Electron-Inertia Effects, *Cambridge University Press*, 1943.
